Journal of Magnetic Resonance 192 (2008) 280–293

Contents lists available at ScienceDirect

Journal of Magnetic Resonance

journal homepage: www.elsevier.com/locate/jmr

NMR measurement of bitumen at different temperatures

Zheng Yang, George J. Hirasaki *

Department of Chemical and Biomolecular Engineering, Rice University, Houston, TX 77005, USA

ARTICLE INFO

Article history:
Received 21 January 2008
Revised 17 March 2008
Available online 20 March 2008

Keywords:
Well logging
Bitumen
Relaxation time
Lognormal distribution
Curie's Law

ABSTRACT

Heavy oil (bitumen) is characterized by its high viscosity and density, which is a major obstacle to both well logging and recovery. Due to the lost information of T_2 relaxation time shorter than echo spacing (TE) and interference of water signal, estimation of heavy oil properties from NMR T_2 measurements is usually problematic. In this work, a new method has been developed to overcome the echo spacing restriction of NMR spectrometer during the application to heavy oil (bitumen). A FID measurement supplemented the start of CPMG. Constrained by its initial magnetization (M_0) estimated from the FID and assuming log normal distribution for bitumen, the corrected T_2 relaxation time of bitumen sample can be obtained from the interpretation of CPMG data. This new method successfully overcomes the TE restriction of the NMR spectrometer and is nearly independent on the TE applied in the measurement.

This method was applied to the measurement at elevated temperatures (8–90 °C). Due to the significant signal-loss within the dead time of FID, the directly extrapolated M_0 of bitumen at relatively lower temperatures (<60 °C) was found to be underestimated. However, resulting from the remarkably lowered viscosity, the extrapolated M_0 of bitumen at over 60 °C can be reasonably assumed to be the real value. In this manner, based on the extrapolation at higher temperatures ($\geqslant$60 °C), the M_0 value of bitumen at lower temperatures (<60 °C) can be corrected by Curie's Law.

Consequently, some important petrophysical properties of bitumen, such as hydrogen index (HI), fluid content and viscosity were evaluated by using corrected T_2.

1. Introduction

Heavy oil and bitumen is characterized by its high viscosity and density, and represent a worldwide known oil reserve of 6 trillion barrels [1,2]. As the conventional oil reserves of the world continue to decline and the exploration and production technologies keep improving, the heavy oil and bitumen deposits have attracted great attention from both the government and the industry, and will be the future of the world oil industry for years to come.

Low field NMR has displayed great potential in many heavy oil well logging cases (California, Venezuela, China) [2]. However, the high oil viscosity still put challenging problems to the NMR logging tools. The echo spacing (TE) limitation of applied NMR logging instrument and the fast relaxation of heavy oil resulting from its high viscosity have combined to make the NMR information (T_2) inevitably get lost during measurements [3–11]. Consequently, estimation of bitumen properties, such as hydrogen index (HI), fluid content and viscosity, based on the captured NMR response is problematic and generally has incorrect TE or sample temperature-dependence.

Kleinberg and Vinegar [3] reported an apparent hydrogen index (HI_{app}) decrease among NMR measurements on some heavy crude oil samples (API gravity <17°) and attributed it to the oil components decaying faster than 1 ms. LaTorraca, et al. [6] investigated on the effects of varying TE on the T_2 distributions and incorporate TE as a parameter into the Vinegar equation (3) to relate the signal-loss (HI_{app} or apparent logarithmic mean T_2, $T_{2,app}$) to the viscosity for heavy oils (>1000 cp).

However, this particular method, which based on the signal-loss in NMR measurement on heavy oils, has inevitable dependence on the value of TE used by the NMR logging tools and need consequent adjustment according to different TE applied. Furthermore, using these signal-loss-based correlations have to combine other logging tools, such as the use of resistivity and density logs for porosity and oil saturation, and estimates of the degree of invasion. The influences from high noise levels on any of these logging tools will bring error into the estimates. More importantly, the essential use of those "apparent" NMR values (HI_{app} or $T_{2,app}$) in this method makes it lose the possibility to develop the ultimate theory-based correlations for oil properties, which undoubtedly depend on the "real" values.

In this work, the new methods for both NMR measurement and subsequent raw data interpretation are developed to correct the T_2 relaxation times of heavy oil (bitumen). The new methods can

* Corresponding author. Fax: +1 713 348 5478.
E-mail address: gjh@rice.edu (G.J. Hirasaki).

1090-7807/$ - see front matter © 2008 Elsevier Inc. All rights reserved.
doi:10.1016/j.jmr.2008.03.007

overcome the echo spacing limitation of NMR spectrometer and have only minor *TE* dependence. Further improvement was also made to eliminate the incorrect temperature-dependence during the application of the new methods at different sample temperatures (8–90 °C). The petrophysical properties, such as hydrogen index, fluid saturation and viscosity are able to be directly estimated from the corrected relaxation times.

2. Equipment and experimental procedures

The major nuclear magnetic resonance (NMR) spectrometer used in this work is a low field Maran-II spectrometer, which is operating at a proton resonance frequency of 2.0 MHz. The effective vertical height of the magnetic field is around 5 cm. The temperature of magnetic field system is controlled at 30 °C with an error of ±0.1 °C.

The heavy oil sample used in this work is froth separated Athabasca bitumen from Alberta, Canada. It consists of bitumen, water and a small amount of clay. The bitumen sample used for the measurements with Maran-II is contained in a glass tube (I.D. 4.66 cm) with a sample height of 3.60 cm. The sample tube was carefully sealed and stored at room temperature.

The NMR measurements were performed at different sample temperatures from 8 to 90 °C. The temperature of magnet was kept at 30 °C for all measurements. Before each measurement, the bitumen sample was placed in a thermal water bath with interested temperature for over 4 h to reach the sample temperature equilibrium. The sample tube was wrapped with four-layer paper insulation during the measurement. A single measurement took less than 1 min. The measurement at each temperature was repeated at least three times to ensure the data reliabilities.

The 90 °C case was employed to demonstrate the temperature change during heating process and NMR measurement. The temperature at the center was used to represent the bitumen sample temperature. As shown in Fig. 1, it only took about 90 min. to heat the bitumen sample from room temperature to 90 °C. The sample was equilibrated for over 4 h. During the subsequent NMR measurement, the sample temperature deviation was 1.6% within 1 min. 90 °C is the highest temperature used in this work and has the largest temperature difference from the magnet temperature (30 °C). According to the results displayed in Fig. 1, it is reasonable to assume that 4-h thermal water bath was enough to reach equilibrium at any interested temperature in this work. And the temperature deviation during the measurement was acceptable.

3. Results

3.1. Regular CPMG measurement on bitumen sample

Regular CPMG measurements were performed on the Athabasca bitumen sample of 30 °C with the Maran-II spectrometer. For the bitumen sample, the applied width of $\pi/2$ pulse was 9.45 μs and that of π pulse was 16.60 μs. Three different echo spacings (*TE*) 0.4, 0.8 and 1.2 ms were applied, respectively. The CPMG raw data were fitted to the standard multi-exponential decay model as follows [12]:

$$M(t) = \sum_i f_i \cdot e^{-\frac{t}{T_{2,i}}} \quad (1)$$

The interpreted T_2 relaxation time distributions of this bitumen sample were shown in Fig. 2. It is clear that, the T_2 distribution of bitumen sample has a strong dependence on the applied echo spacing. When the echo spacing increases, the bitumen peak shifts to the larger relaxation time, while the area of the bitumen peak significantly decreases. It implies that, due to the short T_2 relaxation time (less than 1 ms) of bitumen resulting from its high viscosity (on the order of 10^6 cp), the T_2 of some components of bitumen is even shorter than the echo spacing of the NMR spectrometer. Therefore, as larger echo spacing was applied, more T_2 distribution information of bitumen was lost.

Another observation that can be made from Fig. 2 is that the bitumen signal and water signal are separated clearly in the T_2 relaxation time distribution at 30 °C. The entire signal from the

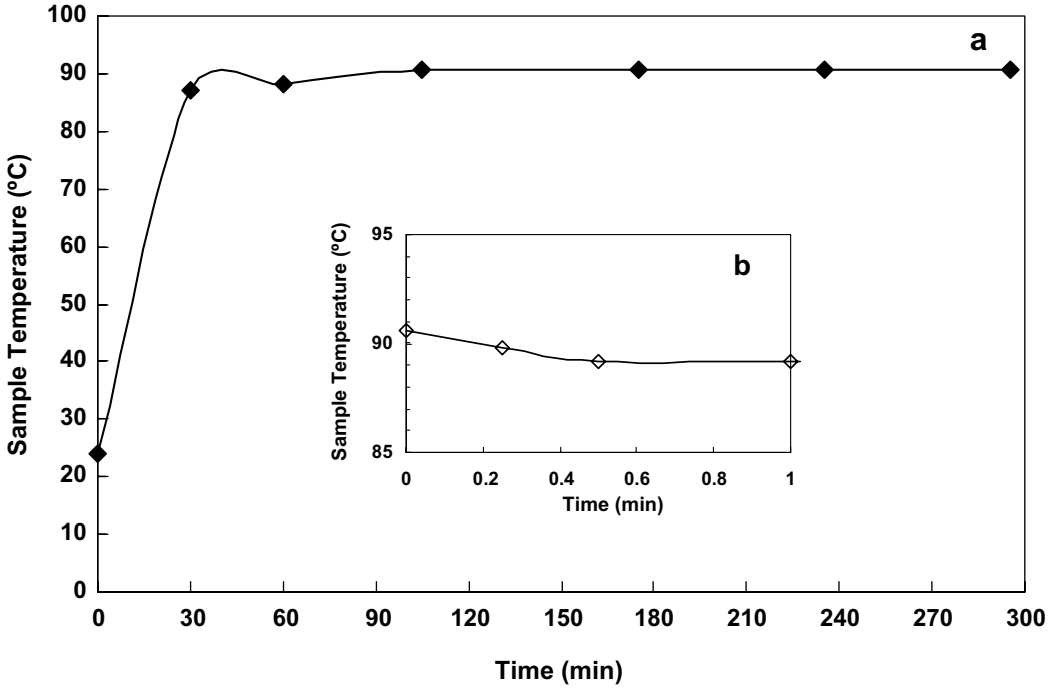

Fig. 1. Temperature change of Athabasca bitumen sample: (a) during heating process, (b) during NMR measurement.

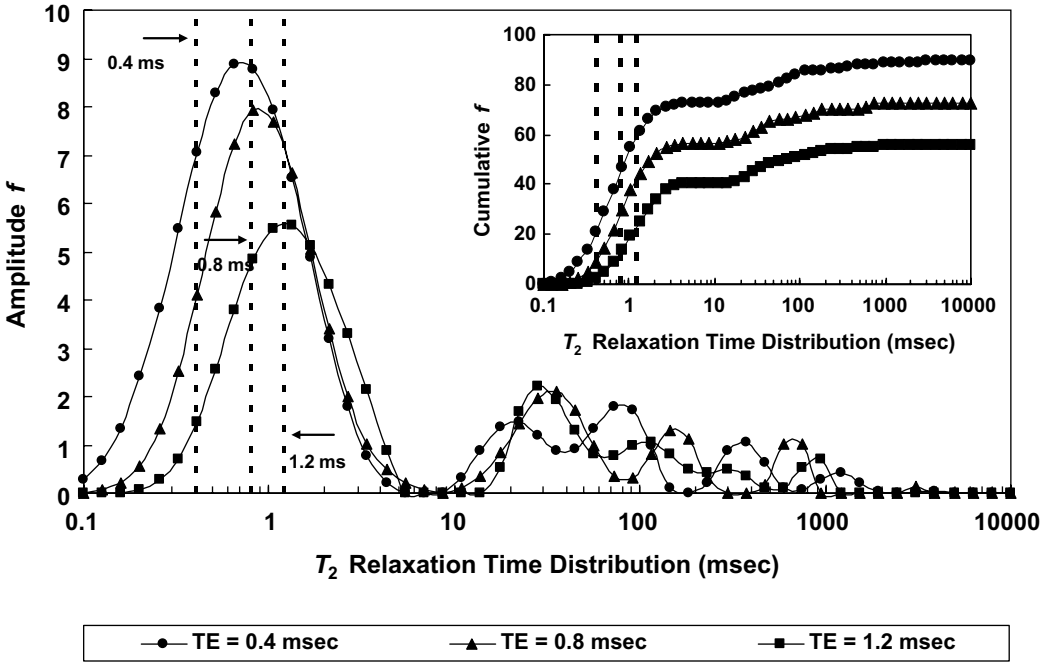

Fig. 2. T_2 distribution of bitumen has strong dependence on echo spacing.

bitumen is found in the first peak from the left of the sample spectra [10]. Thus, in this case, the local minimum after the bitumen peak was employed as the cut-off between oil and water peaks.

The NMR responses (amplitude f) from water and bitumen in the sample are calculated, respectively, and shown in Table 1. We can easily find that, due to the loss of T_2 information shorter than the applied echo spacing, the summation of amplitude from bitumen keeps deceasing when the applied echo spacing increases. On the other hand, the summation of amplitudes from the water response, which can be taken as the indication of area covered by water peaks, only has very slight changes. This implies insensitive response of water to the applied echo spacing, which results from its significantly lower viscosity and larger T_2 relaxation time.

3.2. Improved experimental scheme for correcting T_2 of bitumen

In order to overcome the inevitable echo spacing restriction of Maran-II, a modified scheme for CPMG measurement was developed to correct the T_2 relaxation time of bitumen. In this new scheme, a regular FID was imposed at the start of each CPMG measurement. Then the initial magnetization of the bitumen sample M_0, can be obtained from the extrapolation of FID as shown in Fig. 3.

The transverse relaxation of the measured FID signal follows a first order rate process with a characteristic time constant T_2^* [13]:

$$M(t) = M_0 \cdot e^{-\frac{t}{T_2^*}} \tag{2}$$

Here, M_0 is the initial magnetization of the sample. The constant T_2^* is called transverse relaxation time and affected by the inhomogeneity of the static magnetic field. The time constant describing the decay of the transverse magnetization due to both the spin–spin relaxation of bulk sample (T_2) and the inhomogeneity of the static field is given as:

$$\frac{1}{T_2^*} = \frac{1}{T_{2,b}} + \gamma \cdot \Delta B_0 \tag{3}$$

where $T_{2,b}$ is the intrinsic transverse relaxation time of bitumen, $\gamma \cdot \Delta B_0$ is the inhomogeneity of the static field in unit, kHz.

From the Eqs. (2) and (3), we can see that in order to determine the inhomogeneity of magnetic field, a sample with the property that T_2^* "$T_{2,b}$ must be used. The pure water (deionized), which has a $T_{2,b}$ relaxation time of around 2.9 s, serves this purpose well. Then, the inhomogeneity$\gamma \cdot \Delta B_0$ of the applied magnetic field in this work can be estimated, which is 0.213 kHz as shown in Fig. 3.

Due to the high viscosity of bitumen, the $T_{2,b}$ of bitumen is small and comparable to the inhomogeneity of magnetic field. Therefore, both of the two terms on the right side of Eq. (3) count for the single exponential fitting. Given the inhomogeneity obtained from the FID of pure water (Fig. 3), the estimated T_2 of bitumen is 0.52 ms.

Table 1
NMR response of bitumen sample in regular CPMG

Echo spacing (TE) (ms)	Σf of bitumen in sample	Σf of water in sample	Σf of total bitumen sample
0.4	69.0	17.1	86.1
0.8	57.1	16.8	73.9
1.2	37.9	16.9	54.8

3.3. Improved interpretation method for correcting T_2 of bitumen

Incorporating with the improved experimental scheme described in Section 3.2, a new interpretation method was also developed for interpreting the CPMG raw data of bitumen sample. In this new method, the initial magnetization of bitumen sample, which was obtained from FID measurement, was supplemented to the regular CPMG raw data.

Firstly, the standard multi-exponential model Eq. (1) was still used to interpret the supplemented CPMG data. The case of TE = 0.4 ms was employed as an example and the result of interpretation by using the standard multi-exponential model is shown in Fig. 4. It is clear that, simply using the supplemented CPMG data for interpretation hardly changed the position of bitumen peak. Instead, a long tail showed up at the left side of the bitumen peak as the compensation of the supplemented M_0. In this manner, the estimate of the bitumen T_2 distribution was not improved. A new

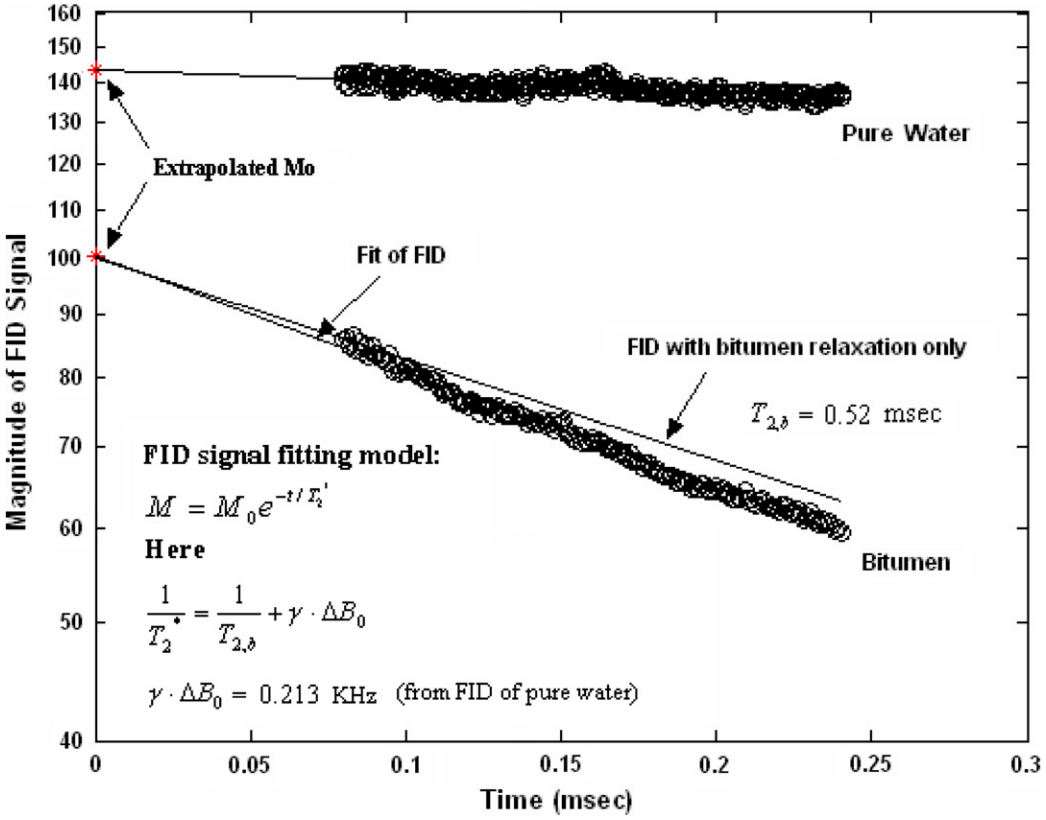

Fig. 3. Estimations of M_0 and T_2 from the extrapolation of FID.

model which is able to better collaborate with the supplementation of CPMG data was in necessity.

The bitumen peaks shown in Fig. 2 are quite symmetric on the semi-logarithmic scale. Furthermore, the logarithmic mean of T_2 is more commonly used in different property correlations. Based on these two points, instead of the standard multi-exponential model, a lognormal distribution model was assumed to represent the T_2 distribution of bitumen. The derivation of this lognormal distribution based model is shown as below.

The multi-exponential model is expressed by Eq. (1). Since it consists of two parts, bitumen and water, it can also be expressed as Eq. (4):

$$M(t) = M_b(t) + M_w(t) = \sum_j f_{b,j} \cdot e^{-\frac{t}{T_{2j}}} + \sum_k f_{w,k} \cdot e^{-\frac{t}{T_{2,k}}} \quad (4)$$

On the right side of Eq. (4), the first term is for bitumen and the second term is for water part in the bitumen sample. Here, we assume the interpretation for water part is correct from standard multi-exponential model and replace the bitumen part in Eq. (4) with a lognormal distribution model. Then, the $M_b(t)$ in Eq. (4) becomes:

$$M_b(t) = f_{b,0} \sum_j g_{b,j} \cdot e^{-\frac{t}{T_{2j}}} \quad (5)$$

In Eq. (5), g_j follows lognormal distribution, as shown in Eq. (6):

$$g_{b,j} = \frac{1}{\sigma\sqrt{2\pi}} \cdot e^{-\frac{\left[\ln(T_{2j}) - \mu\right]^2}{2\sigma^2}} \cdot \Delta \ln(T_{2j}) \quad (6)$$

$$\text{where } \sum_{j=1}^{\infty} g_{b,j} \to 1 \quad (7)$$

It's clear that, in this lognormal distribution model, there are two unknowns, the log-mean T_2 of bitumen, μ, and the standard deviation, σ. In order to optimize the fitting computation, the $\ln(T_{2,j})$ was chosen at μ, $\mu \pm \sigma/2$, $\mu \pm \sigma$, $\mu \pm 3\sigma/2$, $\mu \pm 2\sigma$, $\mu \pm 5\sigma/2$. Then, the T_2 distribution of bitumen could be represented by using eleven points with a lognormal distribution. Thus, in Eq. (6):

$$\Delta \ln(T_{2,j}) = \frac{\sigma}{2} \quad (8)$$

Here, we assume that only bitumen and water in the bitumen sample give NMR response. Therefore, the total response of bitumen $f_{b,0}$ is equal to the difference between the initial magnetization M_0 of bitumen sample and the total NMR response of water part. Then, the $f_{b,0}$ in Eq. (5) can be expressed as:

$$f_{b,0} = M_0 - \sum_k f_{w,k} \quad (9)$$

Finally, the new model, which combines the original multi-exponential model for water part and a lognormal distribution model for bitumen part, can be expressed as below:

$$M(t) = f_{b,0} \sum_j g_{b,j} \cdot e^{-\frac{t}{T_{2j}}} + \sum_k f_{w,k} \cdot e^{-\frac{t}{T_{2,k}}} \quad (10)$$

3.4. Interpretation of CPMG raw data at 30 °C with new model

The M_0 obtained from the FID supplemented the CPMG data. The newly developed model as shown by Eq. (10) was employed to fit the augmented CPMG data at 30 °C.

The fitting results for the CPMG signal obtained with three different echo spacing are shown in Fig. 5(a). The zoom-in for the first 10 ms in Fig. 5(a), which is mainly from the decay of bitumen part, is shown in Fig. 5(b). From Fig. 5, we can find that the new model fit the CPMG raw data of bitumen very well. The interpretations of CPMG data are shown in Fig. 6. The T_2 distributions of bitumen sample obtained from the standard multi-exponential model without specified M_0 are compared with the results from the new mod-

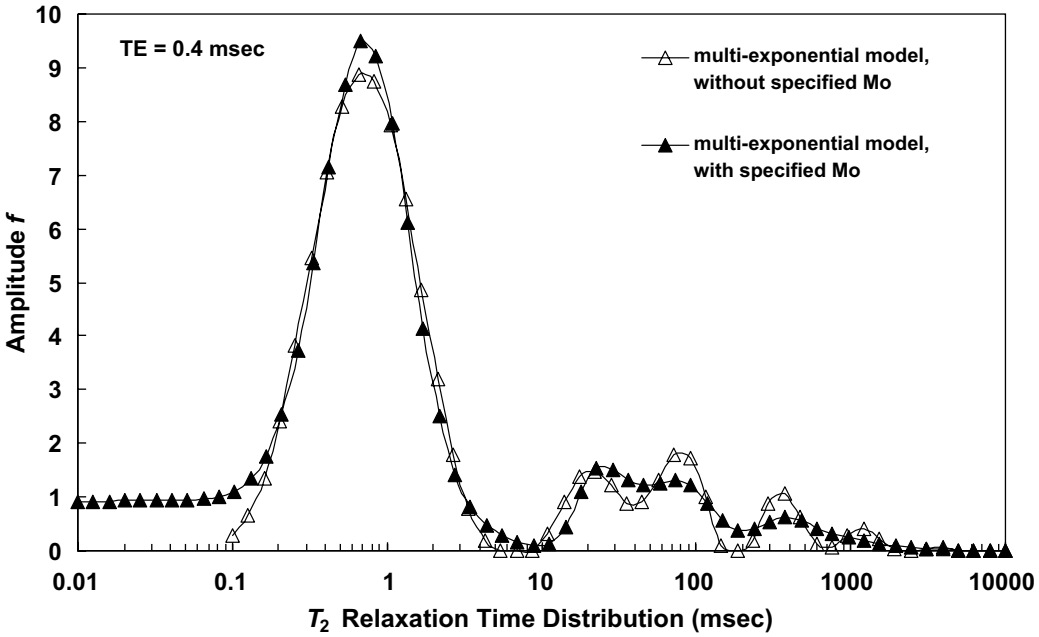

Fig. 4. T_2 distribution of bitumen sample with supplemented M_0. Here, the standard multi-exponential model was used.

el. As displayed in Fig. 6, the T_2 of bitumen estimated by specifying M_0 in CPMG data and assuming lognormal distribution for bitumen are 0.58, 0.56 and 0.54 ms in turn for TE = 0.4, 0.8 and 1.2 ms. However, the corresponding T_2 obtained from the regular CPMG interpretation are 0.74, 0.83, 1.33 ms, respectively. Apparently, the T_2 of bitumen obtained by using the new model are remarkably shorter. More importantly, the corrected T_2 of bitumen has little dependence on echo spacing and is close to the T_2 estimated from FID (0.52 ms).

As shown in the cumulative T_2 distribution in Fig. 6, the area of the bitumen peak is significantly increased by using the new interpretation method. This is due to the compensation for the loss of T_2 information shorter than echo spacing in regular CPMG measurements.

3.5. Application at different sample temperature

It is well known that the temperature of the environment for well logging varies with each application. Therefore, after the successful application in 30 °C case, this new method was also applied for the measurements at different sample temperatures. The temperature range in this work is from 8 to 90 °C, which is adequate for the Canadian bitumen logging. Some important properties of bitumen at different temperatures were evaluated by using its T_2 obtained from the new method.

3.5.1. Calculation method of HI and saturation at different temperatures

The hydrogen index (HI) of a fluid is defined as the proton density of the fluid at any given temperature and pressure divided by the proton density of pure water in standard conditions. It can be expressed as below [15]:

$$HI = \frac{\text{Amount of hydrogen in sample}}{\text{Amount of hydrogen in an equal volume of pure water}} \tag{11}$$

The hydrogen index should be a quantity independent of measurement methods. In this work, the hydrogen index of bitumen can be expressed as Eq. (12).

$$HI_{\mathrm{b}} = \frac{\left(\sum f_{\mathrm{b/b+w}}/V_{\mathrm{b/b+w}}\right)_{\text{at conditions of interest}}}{(T_{\text{standard}}/T_{\text{interest}}) \cdot (M_{0,\mathrm{w}}/V_{\mathrm{t}})_{\text{at standard condition}}} \tag{12}$$

Here,

$\sum f_{\mathrm{b/b+w}}$, sum of f of bitumen part in the bitumen sample;
$\sum f_{\mathrm{w/b+w}}$, sum of f of water part in the bitumen sample;
$M_{0,\mathrm{w}}$, initial magnetization of pure water;
$V_{\mathrm{b/b+w}}$, volume of bitumen part in the bitumen sample;
$V_{\mathrm{w/b+w}}$, volume of water part in the bitumen sample;
V_{t}, total volume of bitumen sample and volume of pure water standard;
T_{standard}, standard temperature of pure water sample;
T_{interest}, interested temperature of pure water sample;

In this work, the total volume of bitumen sample is equal to the volume of pure water as standard, thus the volumes of water and bitumen in the mixture sample can be estimated by Eqs. (13) and (14), respectively:

$$V_{\mathrm{w/b+w}} = V_{\mathrm{t}} \cdot \frac{\left(\sum f_{\mathrm{w/b+w}}\right)_{\text{at conditions of interest}}}{(T_{\text{standard}}/T_{\text{interest}}) \cdot (M_{0,\mathrm{w}})_{\text{at standard condition}}} \tag{13}$$

$$V_{\mathrm{b/b+w}} = V_{\mathrm{t}} - V_{\mathrm{w/b+w}} \tag{14}$$

Another assumption, which was necessary for the investigation on bitumen sample at different temperature, is that the difference of sample volume within our interested temperature range is negligible. Consequently, Eq. (12) becomes,

$$HI_{\mathrm{b}} = \frac{\dfrac{\sum f_{\mathrm{b/b+w}}}{1-\left(\sum f_{\mathrm{w/b+w}}/M_{0,\mathrm{w}}\right)_{\text{at conditions of interest}}}}{(T_{\text{standard}}/T_{\text{interest}}) \cdot (M_{0,\mathrm{w}}/V_{\mathrm{t}})_{\text{at standard condition}}} \tag{15}$$

The equation for calculating water saturation S_{w} can be derived from Eq. (13) and expressed as:

$$S_{\mathrm{w}} = \frac{V_{\mathrm{w/b+w}}}{V_{\mathrm{t}}} = \frac{\left(\sum f_{\mathrm{w/b+w}}\right)_{\text{at conditions of interest}}}{(T_{\text{standard}}/T_{\text{interest}}) \cdot (M_{0,\mathrm{w}})_{\text{at standard condition}}} \tag{16}$$

3.5.2. Investigation on bitumen sample at different temperatures

Besides 30 °C, the bitumen sample was also measured at 8, 20, 40, 50, 60, 70, 80, 90 °C, respectively. The same interpretation

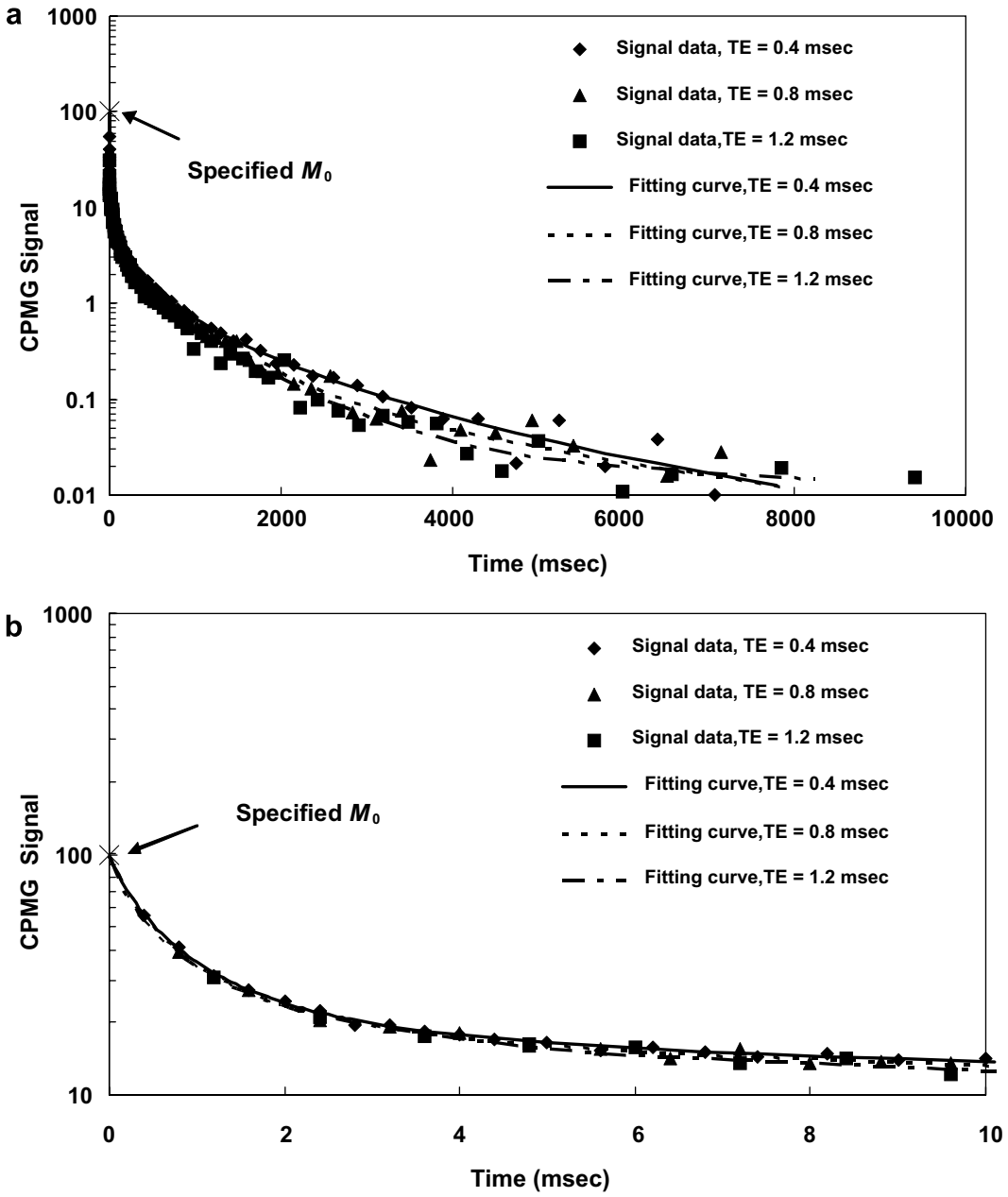

Fig. 5. Fit CPMG data supplemented with M_0 from FID and assume lognormal distribution for bitumen. Here, Fig. 4(b) is Zoom-in for the CPMG fitting of first 10 ms in Fig. 4(a).

method as used in 30 °C case was employed. The *HI* and viscosity of bitumen as well as the water saturation in the sample were estimated by using the T_2 of bitumen obtained from the new method.

3.5.2.1. M_0 from FID at different temperatures. Fig. 7 displays the initial magnetization of bitumen sample at 8, 20, 30, 40, 50, 60 °C, which were estimated from extrapolation of FID. According to Curie's Law [14], when temperature increases, the M_0 of sample should decreases correspondingly. However, within the range from 8 to 60 °C, the extrapolated M_0 of bitumen increases as temperature rises, which is opposite to the Curie's Law's prediction. Moreover, when the temperature is over 40 °C, the extrapolated M_0 becomes very close to each other (indicated by the arrow). The flatter attenuation trend of FID signal at higher temperature is indicative of the significant decrease in sample viscosity when the temperature increases.

Fig. 8 displays the initial magnetization of bitumen sample extrapolated from FID at 60, 70, 80, 90 °C. It's clearly shown that, when temperature is increased over 60 °C, the bitumen M_0 starts decreasing as sample temperature increases. This follows the trend of Curie's Law.

The extrapolated M_0 of bitumen sample at different temperatures shown in Figs. 7 and 8 are also summarized in Fig. 9. (The original Lines 282–286 were removed) The following is the explanation to the unexpected results of extrapolated M_0 at temperature <60 °C shown in Figs. 7 and 8.

The NMR spectrometer, MARAN 2 used in this work has a 80 μs dead time before the first FID signal can be collected (as shown in Figs. 7 and 8). Due to the high viscosity of bitumen, the lost FID signal within the first 80 μs may attenuate much faster than that within the following part. When the temperature decreases, the viscosity of bitumen increases, resulting in an even faster attenuation of FID signal (indicated by the steeper FID at lower temperature). Then, more FID information of bitumen will be lost within the dead time and possible departure from a straight line has a greater effect upon the extrapolation. Thus, M_0 directly extrapo-

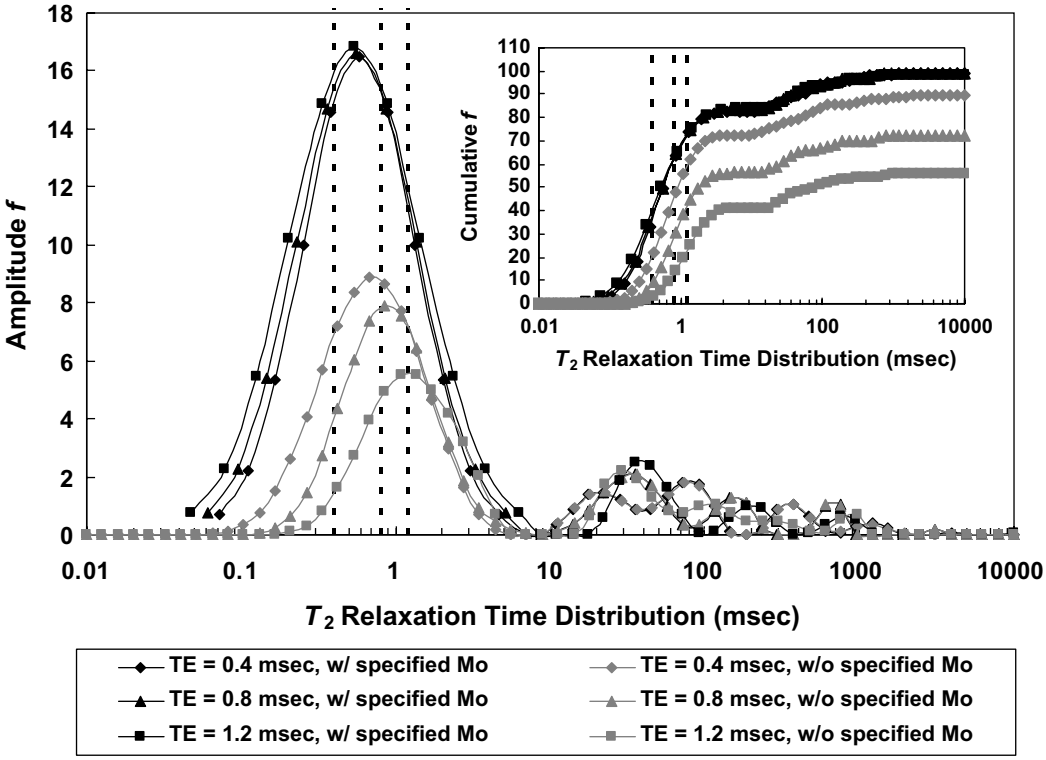

Fig. 6. T_2 distribution of bitumen sample with supplemented M_0 and assuming lognormal distribution for bitumen.

lated from the collected FID data was not accurate for those temperatures <60 °C.

This proposed explanation was supported by the results from the measurement with 20 MHz Bruker minispec spectrometer, which had a dead time of 50 μs rather than the 80 μs of the 2 MHz Maran-II. Fig. 10 displays the Bruker FID signal measured on the same Athabasca bitumen but smaller sample size at 8 and 20 °C. As we expected that, the faster attenuations of bitumen FID signal are observed before 80 μs especially at the lower temperature (8 °C).

The underestimation of the extrapolated M_0 at low temperatures (<60 °C) can be corrected by the Curie's Law. Given a real M_0 value at certain temperature, the M_0 of the same sample at any other temperatures can be predicted by using Curie's Law. When the temperature of bitumen is over 60 °C, the sample viscosity is low enough that complete FID information is assumed to be collected and the extrapolated M_0 decreases with increasing temperature as expected. Therefore, the extrapolated M_0 value at temperature $\geqslant$60 °C can be assumed to be the real values and used as the basis for the Curie's Law correction. As shown in Fig. 9, the difference between the 60 °C-based prediction (solid line) and the 90 °C-based prediction (dashed line) is 3.2%. In this work, the 60 °C-based prediction of M_0 were employed for all the following calculations.

3.5.2.2. Interpretation of CPMG at different temperatures. Supplementing the Curie's Law corrected M_0 into the regular CPMG raw data, the experimental data with specified M_0 at each temperature were fitted to the lognormal distribution based model and the fitting results are shown in Fig. 11. The correspondingly interpreted T_2 distribution of bitumen is shown in Fig. 12 (a).

Fig. 12(b) demonstrates the T_2 distribution of bitumen interpreted by using the apparent M_0. Comparing Fig. 12(a) and (b), we can find that the T_2 distributions of bitumen obtained by simply using the apparent M_0, which directly extrapolated from FID, have remarkable difference from those obtained by using Curie's Law corrected M_0. Both peak area and peak position vary when different M_0 is employed during the interpretation. Moreover, the lower the temperature, the larger the difference.

As shown in Fig. 12 that, at sample temperature <60 °C, the estimated T_2 of bitumen by using the Currie's Law corrected M_0 are uniformly shorter than those estimated with the extrapolated apparent M_0 at each temperature. When the temperature rises over 60 °C, the difference between the two T_2 of bitumen becomes very small.

Furthermore, after using the Curie's Law corrected M_0, the area of bitumen peak at temperature <60 °C is significantly increased. Also, the NMR responses from bitumen, which is indicated by the bitumen peak area, start following the Curie's Law and decreases with increasing temperature.

3.5.2.3. Estimated water saturation in sample at different temperatures. The T_2 distribution of water part in bitumen sample, which was interpreted from the standard multi-exponential model is assumed to be correct. The local minimum after oil peak is employed as the cut-off between oil peak and water response of bitumen sample. In this manner, the water saturation of bitumen sample at each temperature was estimated by using Eq. (16).

As shown by the inset of Fig. 13, the estimated S_w suddenly decreases when the temperature $\geqslant$60 °C. The solid horizontal line is the average value of S_w at 8–50 °C and the corresponding percentage standard deviation is 2.5%.

A proposed explanation to the sudden decrease of S_w at temperature $\geqslant$60 °C is that the cut-off we used in this work to distinguish oil peak and water peaks is not proper in those high temperature cases. When the sample temperature is lower than 60 °C, the bitumen peak is clearly separated from the water peaks. We can simply use the local minimum after the bitumen peak as the cut-off. However, when the sample temperature is raised over 60 °C, due to the comparable T_2 of emulsified water and bitumen, the water peaks

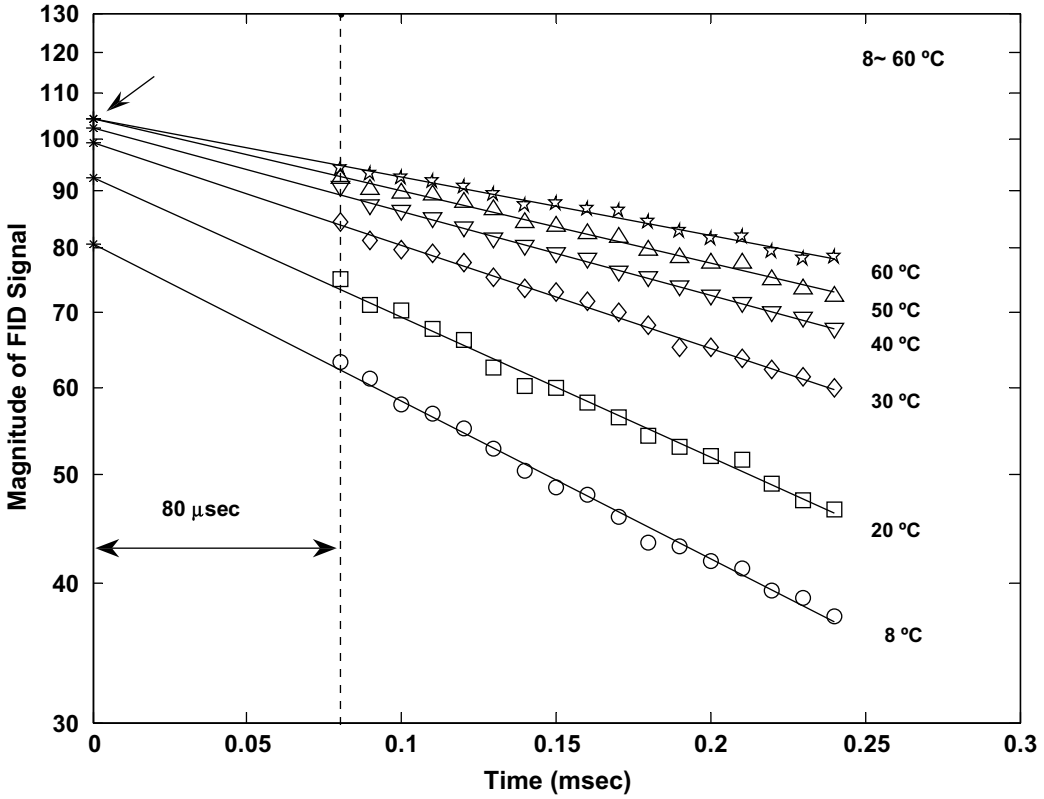

Fig. 7. Extrapolate M_0 of bitumen sample from FID at temperatures: 8–60 °C.

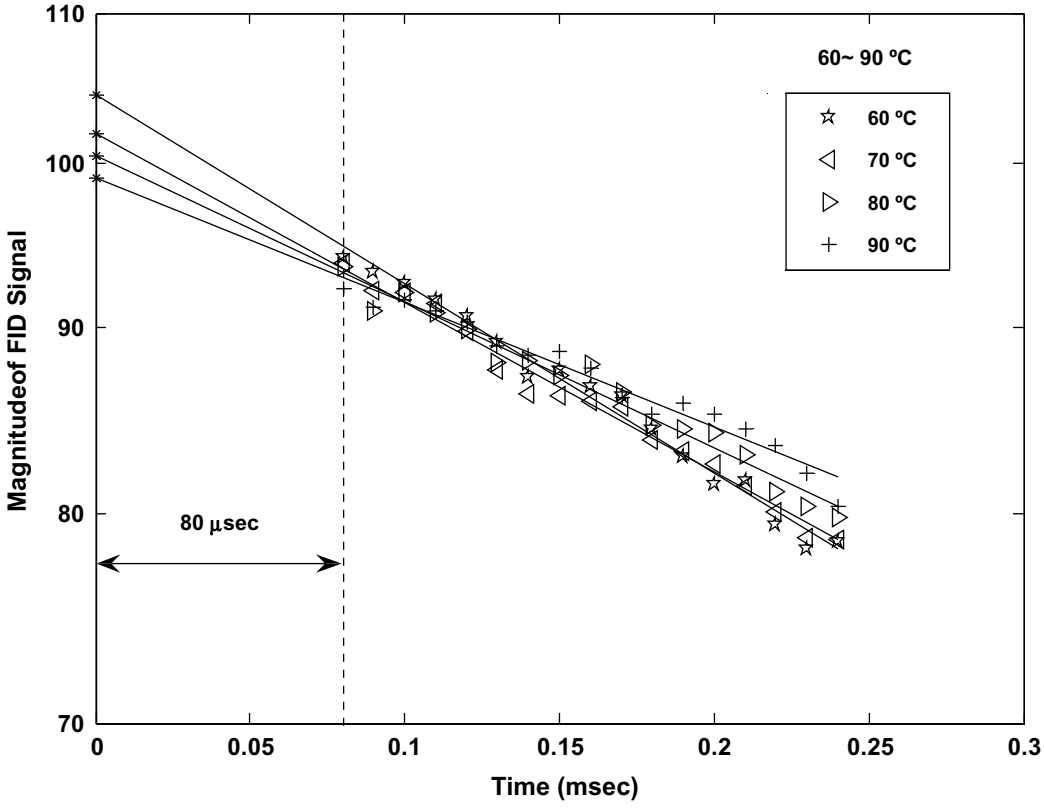

Fig. 8. Extrapolate M_0 of bitumen sample from FID at temperatures: 60–90 °C.

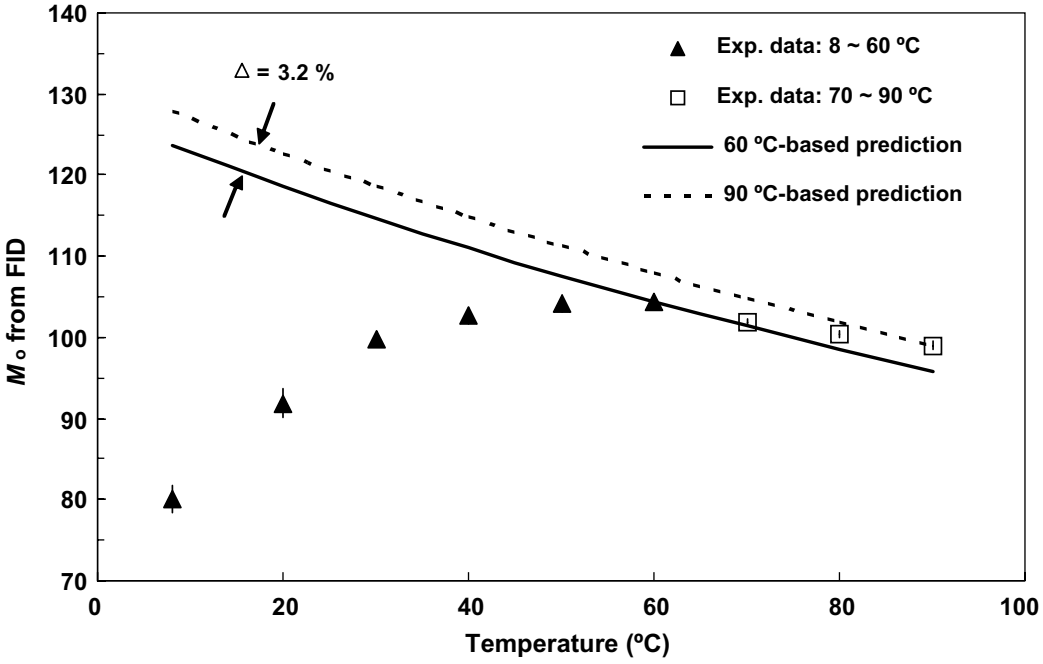

Fig. 9. M_0 of bitumen sample at different temperatures.

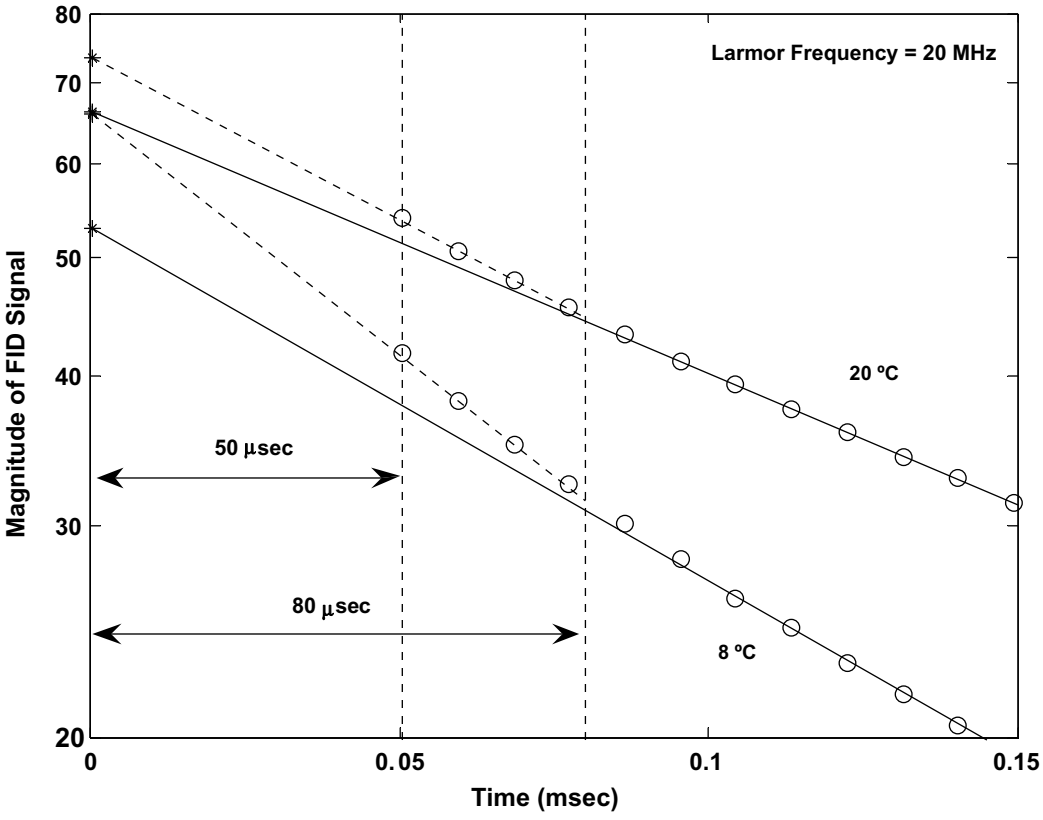

Fig. 10. FID of bitumen sample at 8 and 20 °C. Here, the 20 MHz Bruker minispec NMR spectrometer with a dead time of 50 μs was used. Dashed lines are extrapolation from data 50–80 μs. Solid lines are extrapolation from data $\geqslant$80 μs.

run into the bitumen peak, as shown in Fig. 13. Using the local minimum as the cut-off may not be proper under these conditions.

A more sophisticated oil–water cut-off is necessary in the research on bitumen at high temperatures. In this work, the sample tube was well-sealed. We purposely shuffled the experiment sequence to avoid any unexpected temperature-sequence-dependent results. For example, the 20 °C measurement was performed after the 90 °C one. Based on the experimental data of water satu-

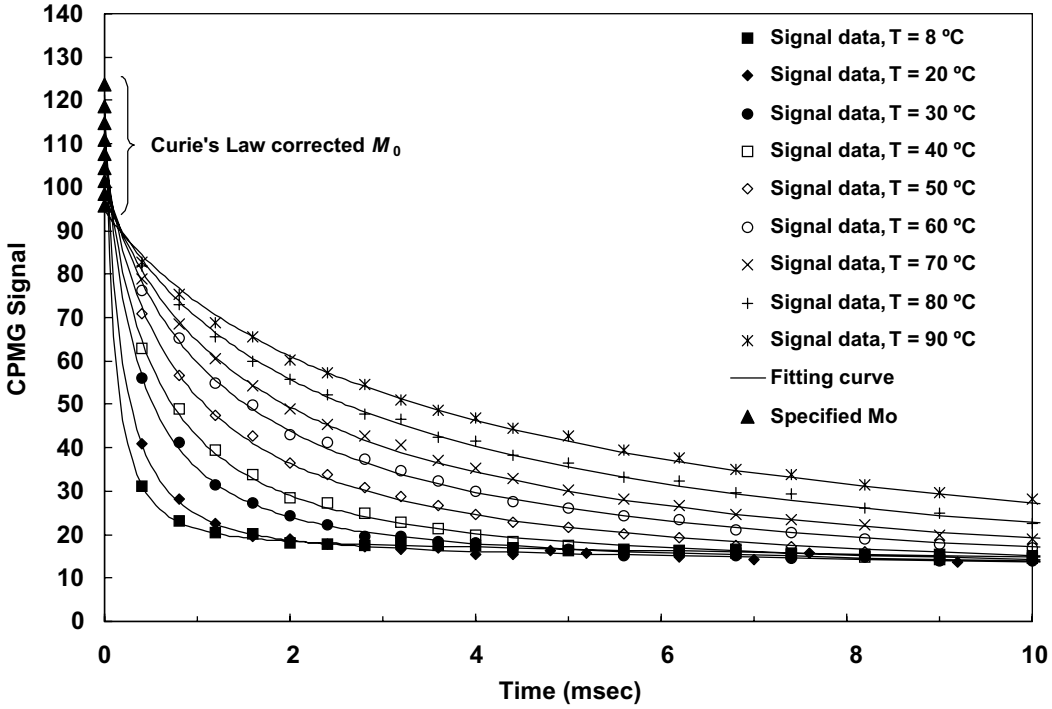

Fig. 11. Fitting supplemented CPMG data by assuming lognormal distribution for bitumen. Here, the specified M_0 is corrected by Curie's Law.

ration shown in Fig. 13, it's reasonable to assume that the real water saturation of bitumen sample does not change within the temperature range of this work.

Therefore, we may be able to use the water saturation data at low temperatures (8–50 °C) to calibrate the cut-off at high temperatures (60–90 °C) in the following research. On the other hand, due to the significant difference between the diffusivities of bitumen and water, we may also use Diffusion Editing measurement [16] to evaluate the NMR response of emulsified water in bitumen samples.

3.5.2.4. Estimated HI of bitumen at different temperatures. The hydrogen index (*HI*) of bitumen at different temperature can be calculated by using Eq. (15) and the results are shown in Fig. 14. It is clear that, when the extrapolated M_0 from FID is not corrected by Curie's Law, the apparent *HI* of bitumen has a temperature-dependence. This is due to the underestimation of apparent M_0 (as shown in Figs. 7 and 9) when sample temperature <60 °C, and the inaccurate cut-off for calculating the water saturation (as shown in Fig. 13) at temperature $\geqslant$60 °C.

However, after the correction for M_0, the incorrect temperature-dependence is eliminated and the bitumenHI stays constant at different temperature. The average value is 0.82 and the percentage standard deviation is only 0.6%.

3.5.2.5. Estimated viscosity of bitumen at different temperatures. A correlation of log-mean T_2 with the ratio of viscosity and temperature, which was derived from alkanes T_1, was developed in previous work of our group [7,8]. As displayed in Fig. 15, given the corrected T_2, the viscosities of bitumen at different temperatures were estimated by using the alkane correlation.

It is clearly shown in Fig. 15 that the viscosity of bitumen estimated from the alkane correlation has significant discrepancy from the experimental value measured by viscometer at low temperatures. As the sample temperature increases, the viscosity of bitumen decreases and the difference between the two viscosity values keeps decreasing. When it reaches 90 °C, the calculated value becomes equal to the experimental value. This means that the alkane correlation, as many other NMR Relaxation Time vs. Viscosity correlations [3,4,6,17], is only good for the oil with relatively low viscosity, but not suitable for those with extremely high viscosity like bitumen. In order to find out the reason responsible for the discrepancy, we need to start from the theoretical basis on highly viscous oil relaxation.

Dead crude oils relax mainly by intramolecular dipole–dipole interactions [18]. By normalizing the relaxation time, viscosity and viscosity/temperature ratio with respect to 2 MHz as shown in Eqs. (17) and (18):

$$T_{1,2N} = \frac{2}{\omega_0} T_{1,2} \tag{17}$$

$$\eta_N = \frac{\omega_0}{2}\eta \tag{18}$$

the intramolecular dipole–dipole interaction model for a rigid spherical molecule can be expressed as follows [8,18]:

$$\frac{1}{T_{1N}} = \frac{W_2 S}{2}\left(\frac{\eta}{T}\right)_N \left\{\frac{2/3}{1+\left[S\left(\frac{\eta}{T}\right)_N\right]^2} + \frac{8/3}{1+\left[2S\left(\frac{\eta}{T}\right)_N\right]^2}\right\} \tag{19}$$

$$\frac{1}{T_{2N}} = \frac{W_2 S}{2}\left(\frac{\eta}{T}\right)_N \left\{1 + \frac{5/3}{1+\left[S\left(\frac{\eta}{T}\right)_N\right]^2} + \frac{2/3}{1+\left[2S\left(\frac{\eta}{T}\right)_N\right]^2}\right\} \tag{20}$$

$$S = \frac{8\pi a^3}{3k} \tag{21}$$

The experimental results between normalized T_1 or T_2 relaxation times and normalized viscosity/temperature ratio are shown in Fig. 16. Also, some literature data are included on the plot [5,18–20]. The 20 MHz data of bitumen in Fig. 16 were obtained from the measurements by using the 20 MHz Bruker minispec NMR spectrometer. The magnet was operating at 40 °C for all experiments and a shorter *TE* (0.184 ms) was employed for the CPMG. The experimental procedure was the same as that used for 2 MHz Maran-II.

As shown in Fig. 16, the frequency-normalized T_1 data of bitumen from this work fall on the same plateau for different Larmor frequencies and follow the curve shown by other literature data.

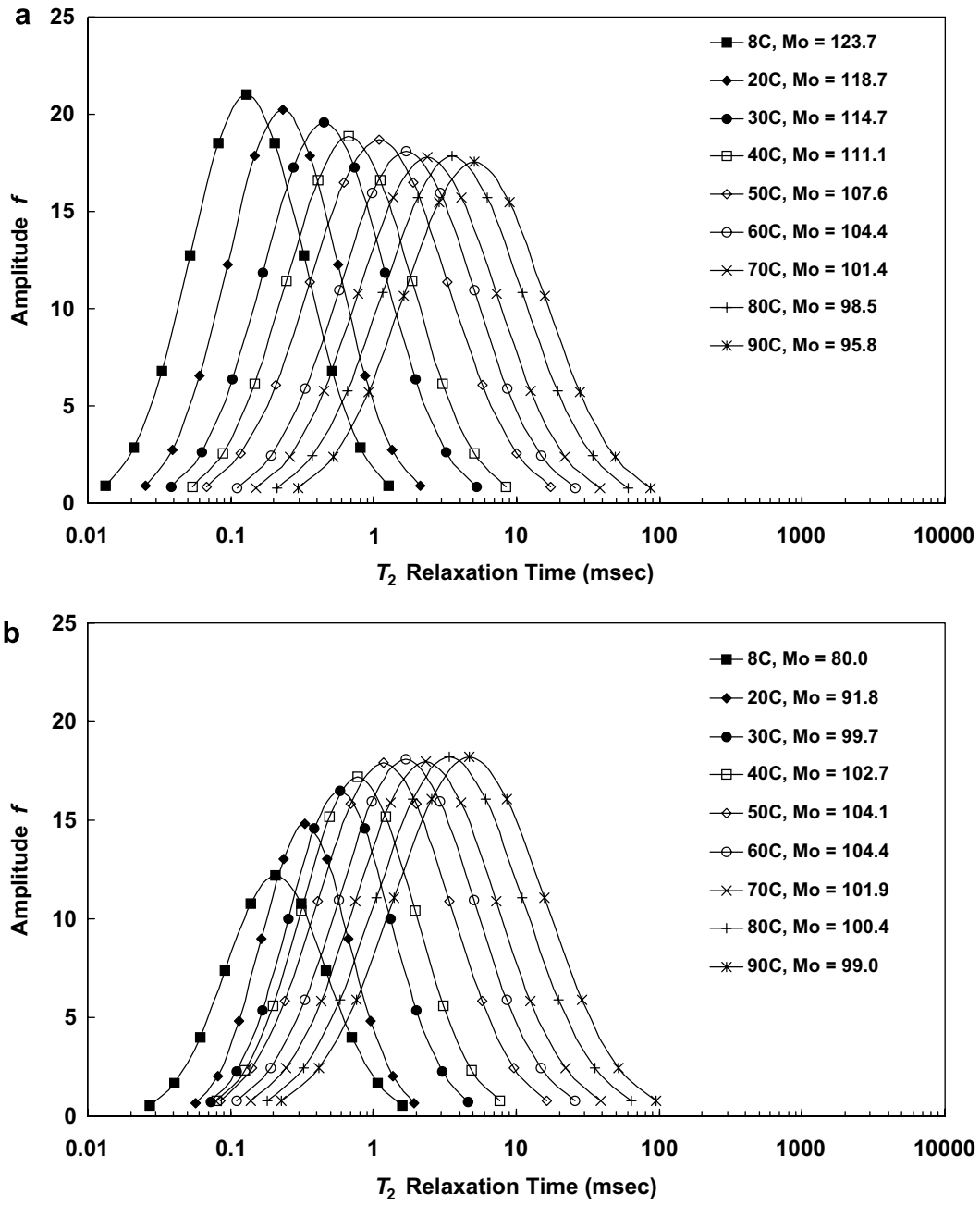

Fig. 12. T_2 distribution of bitumen part obtained by assuming lognormal distribution for bitumen part and specifying M_0. Here, (a) is using Curie's Law corrected M_0; (b) is using apparentM_0 without Curie's Law correction.

Hirasaki et al. [8] and Zhang [18] reported in their work that, the measured T_1 for viscous samples do not follow the theoretical trend, which predicted by the intramolecular dipole–dipole interaction model. The experimental T_1 levels off at high viscosity and reaches a plateau for normalized viscosity/temperature greater than 1 cp/K.

The experimental T_2 continues to shorten with increasing viscosity. Moreover, T_2 is considerably less than T_1 in all cases for heavy oils. As shown in Fig. 16, the measured bitumen normalized T_2 at either Larmor frequency in this work follows the trend of previous literature data. The black solid line in Fig. 16 is from the T_2 correlation by Morriss et al. [4] and the dashed line is from the Alkane correlation [8]. Although the viscosity predictions from the two correlations have difference for light oils, they are quite similar at high viscosities. Viscosity prediction is adaptable for relatively low viscosity crude oils. However, highly viscous samples significantly depart from both of two correlations.

The correlation derived from the intramolecular dipole–dipole interactions model (expressed by Eq. (20)) was also employed to fit the experimental data. The only variable in Eq. (20) is S and its estimated value in this case is 0.082. The fitting results are plotted as the green solid line in Fig. 16. It is clear that the experimental data of heavy oils also have great departure from the dipole–dipole correlation.

In this manner, further work is undergoing and a new correlation will be developed to better correlate T_2 relaxation time and heavy oil viscosity.

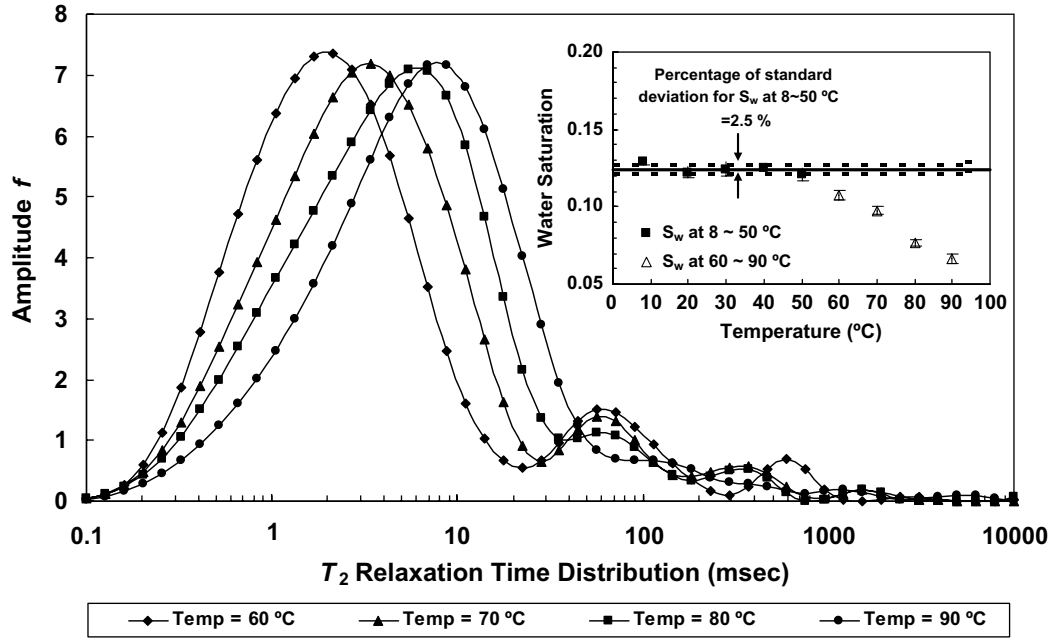

Fig. 13. T_2 distribution of bitumen at temperatures 60, 70, 80, 90 °C, respectively. Here, the CPMG data were interpreted by using the multi-exponential model.

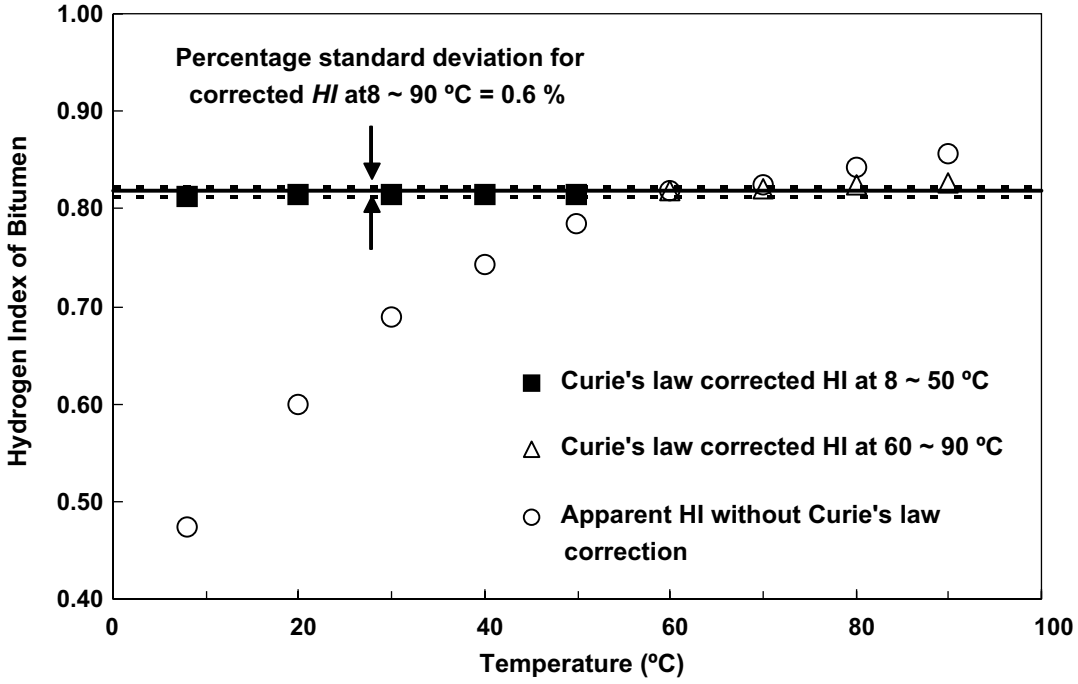

Fig. 14. Hydrogen Index of bitumen at different temperatures.

4. Conclusions

1. The echo spacing restriction of regular CPMG measurement on highly viscous bitumen can be overcome by specifying the M_0 in CPMG raw data and assuming lognormal distribution for bitumen during the interpretation.
2. Apparent M_0 of bitumen from FID at low temperatures (<60 °C) has incorrect dependence on temperature due to the loss of FID signal within the initial decay period. This incorrect temperature-dependence can be corrected by the Curie's Law. Given a correct M_0 value at certain temperature, the M_0 of the same sample at any other temperatures can be predicted by using the equation of Curie's Law.
3. Given Curie's Law corrected M_0 and proper cut-off between oil and water, the hydrogen index (HI) and water saturation (S_w) of bitumen sample can be evaluated by using the method in this work. The estimated HI of Athabasca bitumen is 0.82.
4. The T_1 and T_2 of Athabasca bitumen follow the trend of previous literature data. The existing T_2 vs. viscosity correlations, which are good for the oil with relatively low viscosity, are not suitable for the samples with extremely high viscosity like Canadian bitumen.

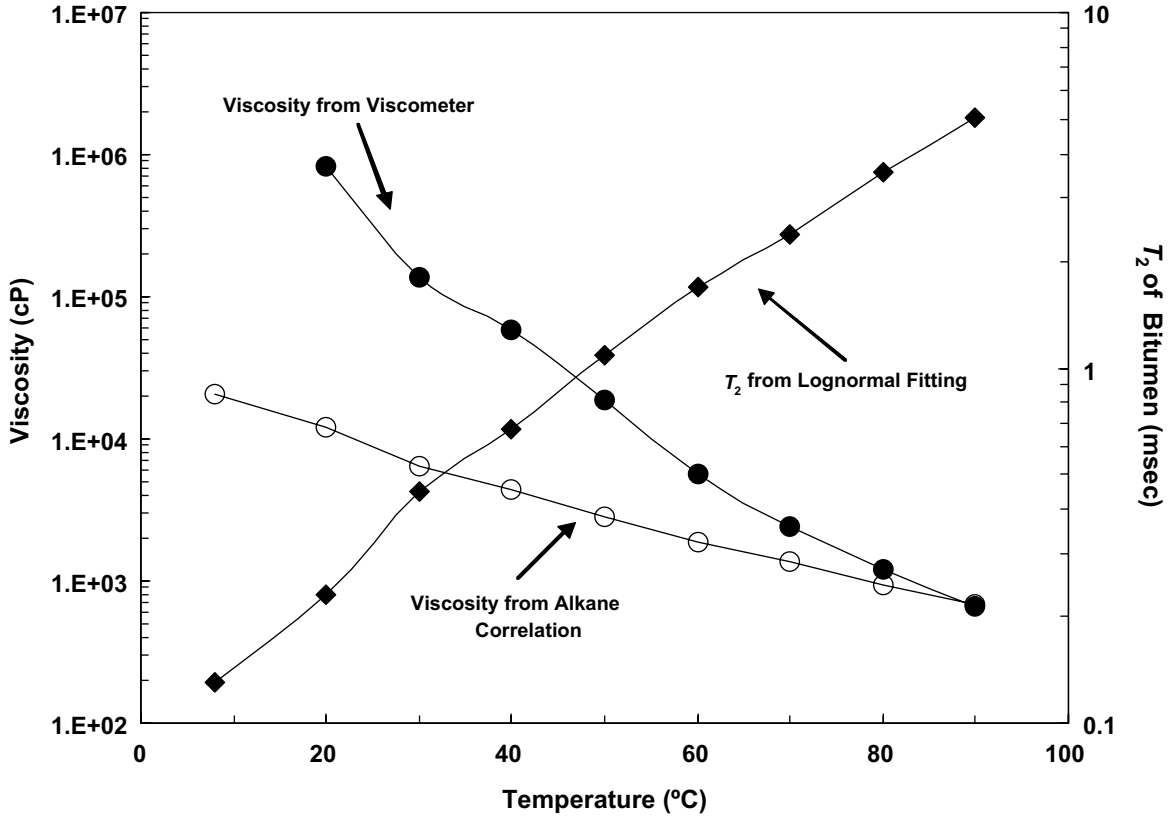

Fig. 15. Comparison on bitumen viscosity from two different methods.

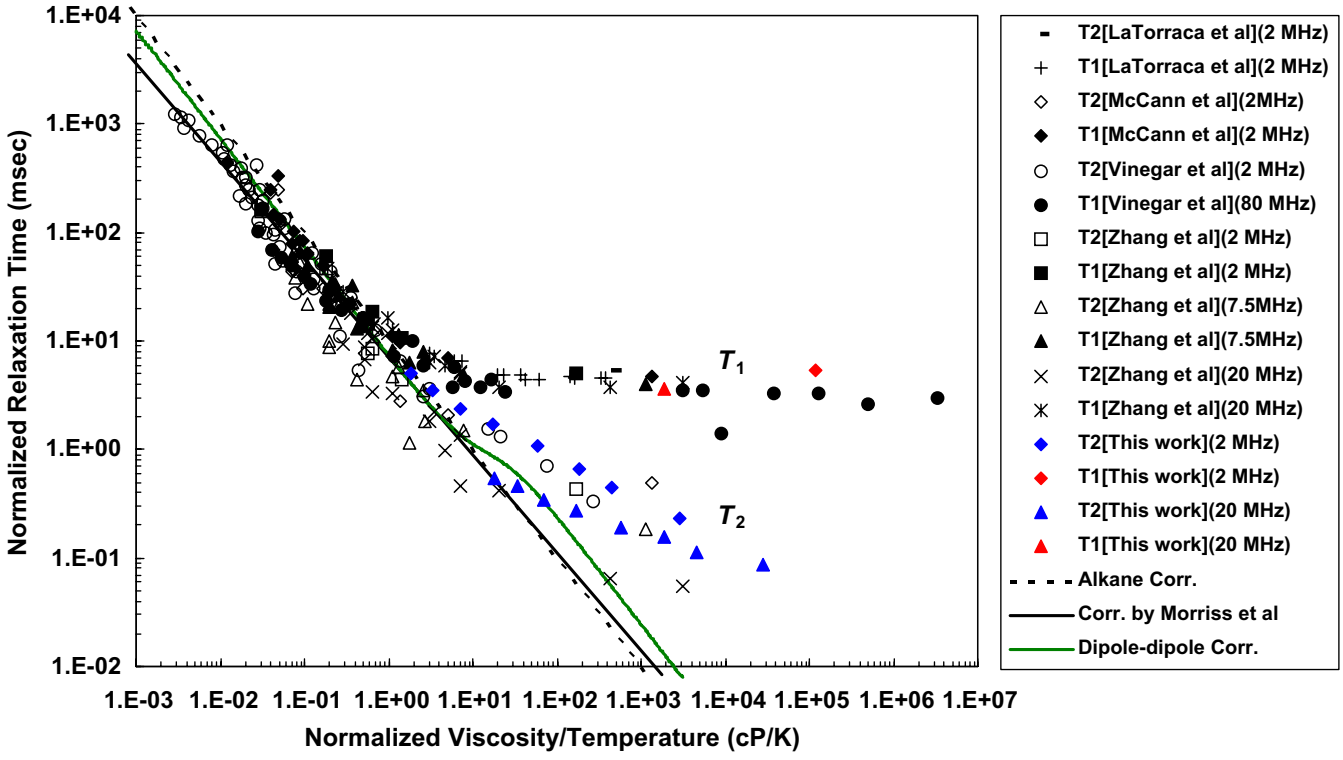

Fig. 16. Relationship between normalized relaxation times and normalized viscosity/temperature ratio.

Acknowledgments

The authors gratefully acknowledge the financial support of NSF, USDOE, and the industrial consortium on Processes in Porous Media at Rice University. The advice of Harold Vinegar is gratefully acknowledged. Zvi Taicher is acknowledged for his use of 20 MHz Bruker spectrometer.

References

[1] J.E. Galford, Combining NMR and conventional logs to determine fluid volumes and oil viscosity in heavy-oil reservoirs, Paper SPE 63257, Society of Petroleum Engineers, presented at the 2000 SPE Annual Technical Conference and Exhibition, Dallas, TX, Oct. 1–4, 2000.

[2] M. Deleersnyder, In-situ heavy-oils viscosity determination using NMR and conventional logs: application to a real example, Paper SPE 86939, Society of Petroleum Engineers, presented at the SPE International Thermal Operations and Heavy Oil Symposium and Western Regional Meeting, Bakersfield, CA, Mar. 16–18, 2004.

[3] R. Kleinberg, H.J. Vinegar, NMR properties of reservoir fluids, The Log Analyst 37 (1996) 20–32.

[4] C.E. Morriss, R. Freedman, C. Straley, M. Johnston, H.J. Vinegar, P.N. Tutunjian, Hydrocarbon saturation and viscosity estimation from NMR logging in the Belridge Diatomite, The Log Analyst 38 (1997) 44–59.

[5] G.A. LaTorraca, K.J. Dunn, P.R. Webber, R.M. Carlson, Low-field NMR determinations of the properties of heavy oils and water-in-oil emulsions, Magnetic Resonance Imaging 16 (1998) 659–662.

[6] G.A. LaTorraca, S.W. Stonard, P.R. Webber, R.M. Carlson, K.J. Dunn, Heavy oil viscosity determination using NMR logs, paper PPP, presented at the 40th SPWLA Annual Logging Symposium, SPWLA, Oslo, Norway, May 30–Jun. 3, 1999.

[7] S.W. Lo, G.J. Hirasaki, W.V. House, R. Kobayashi, Mixing rules and correlations of NMR relaxation time with viscosity, diffusivity and gas/oil ratio of methane/hydrocarbon mixtures, SPEJ March (2002) 24–34.

[8] G.J. Hirasaki, S.W. Lo, Y. Zhang, NMR properties of petroleum reservoir fluids, Magnetic Resonance Imaging 21 (2003) 269–277.

[9] J. Bryan, A. Kantzas, Oil-viscosity predictions from low-field NMR measurements, SPE 89070, SPE Reservoir Evaluation & Engineering 8 (2005) 44–52.

[10] J. Bryan, A. Mai, F. Hum, A. Kantzas, Oil- and water-content measurements in bitumen ore and froth samples using low-field NMR, SPE 97802, SPE Reservoir Evaluation & Engineering 9 (2006) 654–663.

[11] J. Bryan, A. Kantzas, R. Badry, J. Emmerson, T. Hancsicsak, In-situ Viscosity of Heavy Oil: Core and Log Calibrations, Paper 2006-116, presented at the 7th Canadian International Petroleum Conference, Alberta, Canada, June 12-15, 2006.

[12] K.J. Dunn, G.A. LaTorraca, J.L. Warner, D.J. Bergman, On the Calculation and Interpretation of NMR Relaxation Time Distributions, SPE 28367, Society of Petroleum Engineers, The 69th SPE Annual Technical Conference and Exhibition, New Orleans, LA, 1994.

[13] G.R. Coates, L. Xiao, M.G. Prammer, NMR Logging: Principles of Applications, Halliburton Energy Service, Houston, 1999.

[14] B. Cowan, Nuclear Magnetic Resonance and Relaxation, Cambridge University Press, Cambridge, 1997.

[15] K.J. Dunn, D.J. Bergman, C.A. Latorraca, Nuclear Magnetic Resonance Petrophysical and Logging Applications, Pergramon, New York, 2002.

[16] M.D. Hürlimann, L. Venkataramanan, C. Flaum, The diffusion–spin relaxation time distribution function as an experimental probe to characterize fluid mixtures in porous media, Journal of Chemical Physics 117 (2002) 10223–10232.

[17] C. Straley, D. Rossini, A. Vinegar, P.N. Tutunjian, C.E. Morriss, Core analysis by low-field NMR, The Log Analyst 38 (1997) 84–94.

[18] Y. Zhang, Ph.D. Thesis, Rice University, Houston, 2002.

[19] K.E. MaCann, A. Vinegar, G.J. Hirasaki, NMR Analysis of Crude Oil and Pure Hydrocarbon Fluids, (private communication), 1999.

[20] H.J. Vinegar, P.N. Tutunjian, W.A. Edelstein, P.B. Roemer, Whole core analysis by ^{13}C NMR, SPE Formation Evaluation (1991) 183–189.